

Supplementary text, tables and figures for
“Seven newly identified loci for autoimmune
thyroid disease”

Jason D Cooper, Matthew J Simmonds, Neil M Walker, Oliver Burren,
Oliver J Brand, Hui Guo, Chris Wallace, Helen Stevens, Gillian Coleman,
Wellcome Trust Case Control Consortium, Jayne A Franklyn,
John A Todd and Stephen CL Gough

Members of the WTCCC involved in this study

Jan Aerts¹, Tariq Ahmad², Hazel Arbury¹, Anthony Attwood^{1,3,4}, Adam Auton⁵, Stephen G Ball⁶, Anthony J Balmforth⁶, Chris Barnes¹, Jeffrey C Barrett¹, Inês Barroso¹, Anne Barton⁷, Amanda J Bennett⁸, Sanjeev Bhaskar¹, Katarzyna Blaszczyk⁹, John Bowes⁷, Oliver J Brand^{8,10}, Peter S Braund¹¹, Francesca Bredin¹², Gerome Breen^{13,14}, Morris J Brown¹⁵, Ian N Bruce⁷, Jaswinder Bull¹⁶, Oliver S Burren¹⁷, John Burton¹, Jake Byrnes¹⁸, Sian Caesar¹⁹, Niall Cardin⁵, Chris M Clee¹, Alison J Coffey¹, John MC Connell²⁰, Donald F Conrad¹, Jason D Cooper¹⁷, Anna F Dominiczak²⁰, Kate Downes¹⁷, Hazel E Drummond²¹, Darshna Dudakia¹⁶, Andrew Dunham¹, Bernadette Ebbs¹⁶, Diana Eccles²², Sarah Ekins¹, Cathryn Edwards²³, Anna Elliot¹⁶, Paul Emery²⁴, David M Evans²⁵, Gareth Evans²⁶, Steve Eyre⁷, Anne Farmer¹⁴, I Nicol Ferrier²⁷, Edward Flynn⁷, Alistair Forbes²⁸, Liz Forty²⁹, Jayne A Franklyn^{10,30}, Timothy M Frayling², Rachel M Freathy², Eleni Giannoulatou⁵, Polly Gibbs¹⁶, Paul Gilbert⁷, Katherine Gordon-Smith^{19,29}, Emma Gray¹, Elaine Green²⁹, Chris J Groves⁸, Detelina Grozeva²⁹, Rhian Gwilliam¹, Anita Hall¹⁶, Naomi Hammond¹, Matt Hardy¹⁷, Pile Harrison³¹, Neelam Hassanali⁸, Husam Hebaishi¹, Sarah Hines¹⁶, Anne Hinks⁷, Graham A Hitman³², Lynne Hocking³³, Chris Holmes⁵, Eleanor Howard¹, Philip Howard³⁴, Joanna MM Howson¹⁷, Debbie Hughes¹⁶, Sarah Hunt¹, John D Isaacs³⁵, Mahim Jain¹⁸, Derek P Jewell³⁶, Toby Johnson³⁴, Jennifer D Jolley^{3,4}, Ian R Jones²⁹, Lisa A Jones¹⁹, George Kirov²⁹, Cordelia F Langford¹, Hana Lango-Allen², G Mark Lathrop³⁷, James Lee¹², Kate L Lee³⁴, Charlie Lees²¹, Kevin Lewis¹, Cecilia M Lindgren^{8,18}, Meeta Maisuria-Armer¹⁷, Julian Maller¹⁸, John Mansfield³⁸, Jonathan L Marchini⁵, Paul Martin⁷, Dunecan CO Massey¹², Wendy L McArdle³⁹, Peter McGuffin¹⁴, Kirsten E McLay¹, Gil McVean^{5,18}, Alex Mentzer⁴⁰, Michael L Mimmack¹, Ann E Morgan⁴¹, Andrew P Morris¹⁸, Craig Mowat⁴², Patricia B Munroe³⁴, Simon Myers¹⁸, William Newman²⁶, Elaine R Nimmo²¹, Michael C O'Donovan²⁹, Abiodun Onipinla³⁴, Nigel R Ovington¹⁷, Michael J Owen²⁹, Kimmo Palin¹, Aarno Palotie¹, Kirstie Parnel¹², Richard Pearson⁸, David Pernet¹⁶, John RB Perry^{2,18}, Anne Phillips⁴², Vincent Plagnol¹⁷, Natalie J Prescott⁹, Inga Prokopenko^{8,18}, Michael A Quail¹, Suzanne Rafelt¹¹, Nigel W Rayner^{8,18}, David M Reid³³, Anthony Renwick¹⁶, Susan M Ring³⁹, Neil Robertson^{8,18}, Samuel Robson¹, Ellie Russell²⁹, David St Clair¹³, Jennifer G Sambrook^{3,4}, Jeremy D Sanderson⁴⁰, Stephen J Sawcer⁴³, Helen Schuilenburg¹⁷, Carol E Scott¹, Richard Scott¹⁶, Sheila Seal¹⁶, Sue Shaw-Hawkins³⁴, Beverley M Shields², Matthew J Simmonds^{8,10}, Debbie J Smyth¹⁷, Elilan Somaskantharajah¹, Katarina Spanova¹⁶, Sophia Steer⁴⁴, Jonathan Stephens^{3,4}, Helen E Stevens¹⁷, Kathy Stirrups¹, Millicent A Stone^{45,46}, David P Strachan⁴⁷, Zhan Su⁵, Deborah PM Symmons⁷, John R Thompson⁴⁸, Wendy Thomson⁷, Martin D Tobin⁴⁸, Mary E Travers⁸, Clare Turnbull¹⁶, Damjan Vukcevic¹⁸, Louise V Wain⁴⁸, Mark Walker⁴⁹, Neil M Walker¹⁷, Chris Wallace¹⁷, Margaret Warren-Perry¹⁶, Nicholas A Watkins^{3,4}, John Webster⁵⁰, Michael N Weedon², Anthony G Wilson⁵¹, Matthew Woodburn¹⁷, B Paul Wordsworth⁵², Chris Yau⁵, Allan H Young^{27,53}, Eleftheria Zeggini¹, Matthew A Brown^{52,54}, Paul R Burton⁴⁸, Mark J Caulfield³⁴, Alastair Compston⁴³, Martin Farrall⁵⁵, Stephen CL Gough^{8,10,30}, Alistair S Hall⁶, Andrew T Hattersley^{2,56}, Adrian VS Hill¹⁸, Christopher G Mathew⁹, Marcus Pembrey⁵⁷, Jack Satsangi²¹, Michael R Stratton^{1,16}, Jane Worthington⁷, Matthew E Hurles¹, Audrey Duncanson⁵⁸, Willem H Ouwehand^{1,3,4}, Miles Parkes¹², Nazneen Rahman¹⁶, John A Todd¹⁷, Nilesh J Samani^{1,59}, Dominic P Kwiatkowski^{1,18}, Mark I McCarthy^{8,18,60}, Nick Craddock²⁹, Panos Deloukas¹, Peter Donnelly^{5,18}.

- ¹ The Wellcome Trust Sanger Institute, Wellcome Trust Genome Campus, Hinxton, Cambridge, CB10 1SA UK.
- ² Genetics of Complex Traits, Peninsula College of Medicine and Dentistry University of Exeter, EX1 2LU, UK.
- ³ Department of Haematology, University of Cambridge, Long Road, Cambridge, CB2 0PT, UK.
- ⁴ National Health Service Blood and Transplant, Cambridge Centre, Long Road, Cambridge CB2 0PT, UK.
- ⁵ Department of Statistics, University of Oxford, 1 South Parks Road, Oxford, OX1 3TG, UK.
- ⁶ Multidisciplinary Cardiovascular Research Centre (MCRC), Leeds Institute of Genetics, Health and Therapeutics (LIGHT), University of Leeds, Leeds, LS2 9JT, UK.
- ⁷ arc Epidemiology Unit, Stopford Building, University of Manchester, Oxford Road, Manchester, M13 9PT, UK.
- ⁸ Oxford Centre for Diabetes, Endocrinology and Medicine, University of Oxford, Churchill Hospital, Oxford OX3 7LJ, UK.
- ⁹ Department of Medical and Molecular Genetics, King's College London School of Medicine, 8th Floor Guy's Tower, Guy's Hospital, London, SE1 9RT, UK.
- ¹⁰ Centre for Endocrinology, Diabetes and Metabolism, Institute of Biomedical Research, University of Birmingham, Birmingham, B15 2TT, UK.
- ¹¹ Department of Cardiovascular Sciences, University of Leicester, Glenfield Hospital, Groby Road, Leicester LE3 9QP, UK.
- ¹² IBD Genetics Research Group, Addenbrooke's Hospital, Cambridge, CB2 0QQ, UK.
- ¹³ University of Aberdeen, Institute of Medical Sciences, Foresterhill, Aberdeen AB25 2ZD, UK.
- ¹⁴ SGDP, The Institute of Psychiatry, King's College London, De Crespigny Park, Denmark Hill, London SE5 8AF, UK.
- ¹⁵ Clinical Pharmacology Unit, University of Cambridge, Addenbrookes Hospital, Hills Road, Cambridge CB2 2QQ, UK.
- ¹⁶ Section of Cancer Genetics, Institute of Cancer Research, 15 Cotswold Road, Sutton SM2 5NG, UK.
- ¹⁷ Juvenile Diabetes Research Foundation/Wellcome Trust Diabetes and Inflammation

Laboratory, Department of Medical Genetics, Cambridge Institute for Medical Research, University of Cambridge, Wellcome Trust/MRC Building, Cambridge CB2 0XY, UK.

¹⁸ The Wellcome Trust Centre for Human Genetics, University of Oxford, Roosevelt Drive, Oxford OX3 7BN, UK.

¹⁹ Department of Psychiatry, University of Birmingham, National Centre for Mental Health, 25 Vincent Drive, Birmingham, B15 2FG, UK.

²⁰ BHF Glasgow Cardiovascular Research Centre, University of Glasgow, 126 University Place, Glasgow, G12 8TA, UK.

²¹ Gastrointestinal Unit, Division of Medical Sciences, School of Molecular and Clinical Medicine, University of Edinburgh, Western General Hospital, Edinburgh EH4 2XU, UK.

²² Academic Unit of Genetic Medicine, University of Southampton, Southampton, UK.

²³ Endoscopy Regional Training Unit, Torbay Hospital, Torbay TQ2 7AA, UK.

²⁴ Academic Unit of Musculoskeletal Disease, University of Leeds, Chapel Allerton Hospital, Leeds, West Yorkshire LS7 4SA, UK.

²⁵ MRC Centre for Causal Analyses in Translational Epidemiology, Department of Social Medicine, University of Bristol, Bristol, BS8 2BN, UK.

²⁶ Department of Medical Genetics, Manchester Academic Health Science Centre (MAHSC), University of Manchester, Manchester M13 0JH, UK.

²⁷ School of Neurology, Neurobiology and Psychiatry, Royal Victoria Infirmary, Queen Victoria Road, Newcastle upon Tyne, NE1 4LP, UK.

²⁸ Institute for Digestive Diseases, University College London Hospitals Trust, London NW1 2BU, UK.

²⁹ MRC Centre for Neuropsychiatric Genetics and Genomics, School of Medicine, Cardiff University, Heath Park, Cardiff, CF14 4XN, UK.

³⁰ University Hospital Birmingham NHS Foundation Trust, Birmingham, B15 2TT, UK.

³¹ University of Oxford, Institute of Musculoskeletal Sciences, Botnar Research Centre, Oxford, OX3 7LD, UK.

³² Centre for Diabetes and Metabolic Medicine, Barts and The London, Royal London Hospital, Whitechapel, London, E1 1BB, UK.

³³ Bone Research Group, Department of Medicine and Therapeutics, University of Aberdeen, Aberdeen, AB25 2ZD, UK.

- ³⁴ Clinical Pharmacology and Barts and The London Genome Centre, William Harvey Research Institute, Barts and The London School of Medicine and Dentistry, Queen Mary University of London, Charterhouse Square, London EC1M 6BQ, UK.
- ³⁵ Institute of Cellular Medicine, Musculoskeletal Research Group, 4th Floor, Catherine Cookson Building, The Medical School, Framlington Place, Newcastle upon Tyne, NE2 4HH, UK.
- ³⁶ Gastroenterology Unit, Radcliffe Infirmary, University of Oxford, Oxford, OX2 6HE, UK.
- ³⁷ Centre National de Genotypage, 2, Rue Gaston Cremieux, Evry, Paris 91057, France.
- ³⁸ Department of Gastroenterology & Hepatology, University of Newcastle upon Tyne, Royal Victoria Infirmary, Newcastle upon Tyne NE1 4LP, UK.
- ³⁹ ALSPAC Laboratory, Department of Social Medicine, University of Bristol, BS8 2BN, UK.
- ⁴⁰ Division of Nutritional Sciences, King's College London School of Biomedical and Health Sciences, London SE1 9NH, UK.
- ⁴¹ NIHR-Leeds Musculoskeletal Biomedical Research Unit, University of Leeds, Chapel Allerton Hospital, Leeds, West Yorkshire LS7 4SA, UK.
- ⁴² Department of General Internal Medicine, Ninewells Hospital and Medical School, Ninewells Avenue, Dundee DD1 9SY, UK.
- ⁴³ Department of Clinical Neurosciences, University of Cambridge, Addenbrooke's Hospital, Hills Road, Cambridge, CB2 2QQ, UK.
- ⁴⁴ Clinical and Academic Rheumatology, Kings College Hospital National Health Service Foundation Trust, Denmark Hill, London SE5 9RS, UK.
- ⁴⁵ University of Toronto, St. Michael's Hospital, 30 Bond Street, Toronto, Ontario M5B 1W8, Canada.
- ⁴⁶ University of Bath, Claverdon, Norwood House, Room 5.11a Bath Somerset BA2 7AY, UK.
- ⁴⁷ Division of Community Health Sciences, St George's, University of London, London SW17 0RE, UK.
- ⁴⁸ Departments of Health Sciences and Genetics, University of Leicester, 217 Adrian Building, University Road, Leicester, LE1 7RH, UK.
- ⁴⁹ Diabetes Research Group, School of Clinical Medical Sciences, Newcastle University, Framlington Place, Newcastle upon Tyne NE2 4HH, UK.

⁵⁰ Medicine and Therapeutics, Aberdeen Royal Infirmary, Foresterhill, Aberdeen, Grampian AB9 2ZB, UK.

⁵¹ School of Medicine and Biomedical Sciences, University of Sheffield, Sheffield, S10 2JF, UK.

⁵² Nuffield Department of Orthopaedics, Rheumatology and Musculoskeletal Sciences, Nuffield Orthopaedic Centre, University of Oxford, Windmill Road, Headington, Oxford, OX3 7LD, UK.

⁵³ UBC Institute of Mental Health, 430-5950 University Boulevard Vancouver, British Columbia, V6T 1Z3, Canada.

Supplementary Tables

Table S1: Evidence for reported AITD non-HLA susceptibility loci. Genotype signal intensity cluster plots have been examined visually. Note that the AITD locus *SCGB3A2/5q32* was not included on the ImmunoChip. Hashimoto's thyroiditis (HT), Graves' disease (GD), minor allele frequency (MAF), odds ratio (OR) and confidence interval (CI).

| Gene Karyotype band | Most associated SNP | MAF in in controls | 2,285 GD patients and 9,364 controls | | 462 HT patients and 9,364 controls | | Heterogeneity in disease association <i>P</i> -value | 2,282 GD, 451 HT and 9,364 controls | |
|-----------------------------|------------------------|-----------------------|---|------------------------|---------------------------------------|------------------------|---|--|------------------------|
| | | | OR (95% CI) | <i>P</i> -value | OR (95% CI) | <i>P</i> -value | | OR (95% CI) | <i>P</i> -value |
| <i>PTPN22</i> 1p13.2 | rs2476601 G>A | 0.0962 | 1.55 (1.41-1.71) | 4.03x10 ⁻¹⁶ | 2.02 (1.69-2.41) | 3.74x10 ⁻¹⁵ | †6.76x10 ⁻³ | 1.63 (1.49-1.78) | 9.69x10 ⁻²³ |
| <i>FCRL3</i> 1q23.1 | rs7522061 T>C | 0.480 | 1.16 (1.08-1.23) | 1.08x10 ⁻⁵ | 1.03 (0.90-1.18) | 0.634 | 0.122 | 1.14 (1.07-1.21) | 2.36x10 ⁻⁵ |
| <i>CTLA4/ICOS</i> 2q33.2 | rs11571297 G>A | 0.493 | 0.72 (0.67-0.77) | 2.81x10 ⁻²³ | 0.82 (0.72-0.94) | 3.21x10 ⁻³ | 0.0682 | 0.73 (0.69-0.78) | 2.09x10 ⁻²³ |
| <i>IL2RA</i> 10p15.1 | rs706779 A>G | 0.467 | 0.85 (0.80-0.91) | 2.27x10 ⁻⁶ | 0.84 (0.74-0.96) | 0.0125 | 0.858 | 0.85 (0.80-0.91) | 2.69x10 ⁻⁷ |
| <i>TSHR</i> 14q31.1 | rs2300519 T>A | 0.380 | 1.54 (1.44-1.64) | 1.34x10 ⁻³⁸ | 0.93 (0.81-1.07) | 0.295 | 4.64x10 ⁻¹² | | |

†Assuming 13 [8 (Table 1) and 5 (Table S1)] independent tests, the adjusted *P*-value was 3.85x10⁻³ for the 0.05 level of significance based on a Bonferroni correction for multiple testing.

Table S2: A summary of SNPs that show large allele frequency differences ($P < 1.12 \times 10^{-6}$) between controls from the 12 geographical regions of Great Britain (Materials and Methods). Genotype signal intensity cluster plots have been examined visually for these highly differential SNPs (two SNPs were dropped rs2310187/2q12.1 and rs12210050/6p25.3). We note that the most significant *LCT* SNP, rs2236783/2q21.3 ($P = 1.41 \times 10^{-5}$), was above the threshold *P*-value. Positions are in NCBI build 36 co-ordinates. distance in base pairs (dist).

| Chromosome | Gene | Reported SNP | Position (base pairs) | P-value |
|------------|--|-----------------|-----------------------|----------|
| 2 | IL1R2(dist=99131),IL1R1(dist=26387) | rs12470623 | 102110447 | 1.52e-07 |
| 2 | IL1R2(dist=101821),IL1R1(dist=23697) | rs6752379 | 102113137 | 1.52e-07 |
| 2 | IL1R2(dist=116654),IL1R1(dist=8864) | rs11123911 | 102127970 | 1.51e-07 |
| 2 | IL1R2(dist=118953),IL1R1(dist=6565) | rs13035227 | 102130269 | 1.04e-06 |
| 2 | IL1R2(dist=119894),IL1R1(dist=5624) | rs6754776 | 102131210 | 1.09e-06 |
| 2 | IL1R1 | rs871658 | 102138297 | 1.07e-06 |
| 2 | RAB3GAP1 | rs7570971 | 135554376 | 9.01e-09 |
| 2 | RAB3GAP1 | rs6730157 | 135623558 | 4.32e-09 |
| 2 | RAB3GAP1(dist=26518),ZRANB3(dist=2777) | rs1375131 | 135671267 | 2.22e-09 |
| 2 | ZRANB3 | rs1561277 | 135808531 | 3.49e-07 |
| 2 | R3HDM1 | rs56369224 | 136045360 | 5.29e-08 |
| 2 | R3HDM1 | rs12465802 | 136097818 | 1.10e-07 |
| 2 | MCM6 | rs4988235 | 136325116 | 2.54e-09 |
| 2 | MCM6 | rs182549 | 136333224 | 6.56e-09 |
| 2 | DARS | rs6754311 | 136424452 | 4.49e-09 |
| 2 | DARS | rs12615624 | 136438073 | 2.74e-07 |
| 4 | TLR1(dist=9090),TLR6(dist=9827) | rs4833103 | 38491897 | 2.40e-10 |
| 6 | IRF4 | rs12203592 | 341321 | 4.31e-22 |
| 6 | IRF4(dist=9838),EXOC2(dist=63857) | rs62389423 | 366281 | 1.44e-15 |
| 6 | IRF4(dist=11188),EXOC2(dist=62507) | rs62389424 | 367631 | 3.69e-15 |
| 6 | IRF4(dist=13472),EXOC2(dist=60223) | rs9405661 | 369915 | 1.09e-06 |
| 6 | IRF4(dist=20607),EXOC2(dist=53088) | rs6925797 | 377050 | 1.52e-07 |
| 16 | ZNF764 | imm_16_30477512 | 30477512 | 1.67e-07 |
| 16 | ZNF785 | rs9934806 | 30500560 | 1.02e-07 |
| 16 | ZNF689 | rs8063005 | 30525199 | 9.15e-08 |
| 16 | PHKG2 | rs72793380 | 30666244 | 5.76e-07 |

Supplementary Figures

Figure S1: Single-locus 1-df Cochran-Armitage trend test results at the recently reported novel AITD susceptibility locus 6q27 (1). The most disease associated SNP, imm-6-167338101 ($P = 1.6 \times 10^{-7}$ in HT and GD patients/controls; Table 1), was located within *FGFR10P*. The top panel — GD patients and controls; the middle panel — HT patients and controls; and, the bottom panel — GD and HT patients and controls.

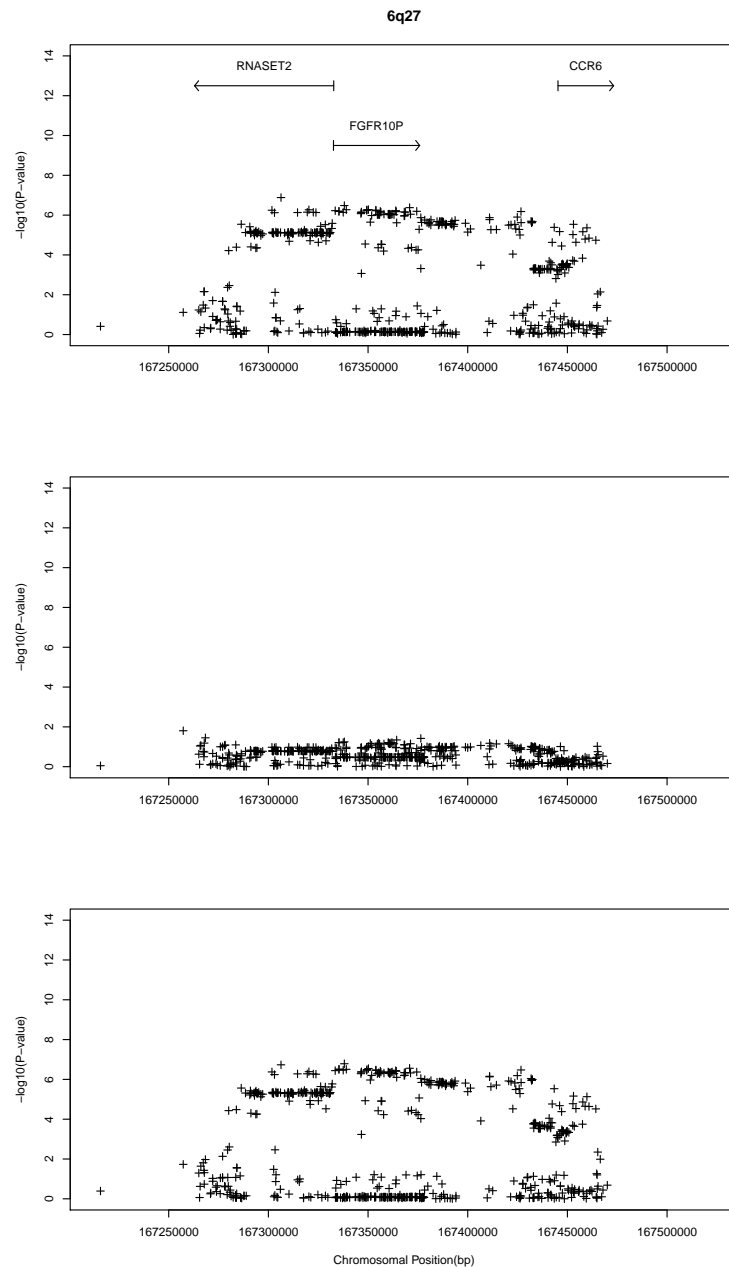


Figure S2: Single-locus 1-df Cochran-Armitage trend test results at the novel AITD susceptibility locus 1q36.32. The most disease associated SNP, rs2843403 ($P = 7.9 \times 10^{-7}$ in GD patients/controls; Table 1), was located within *MMEL1*. The top panel — GD patients and controls; the middle panel — HT patients and controls; and, the bottom panel — GD and HT patients and controls.

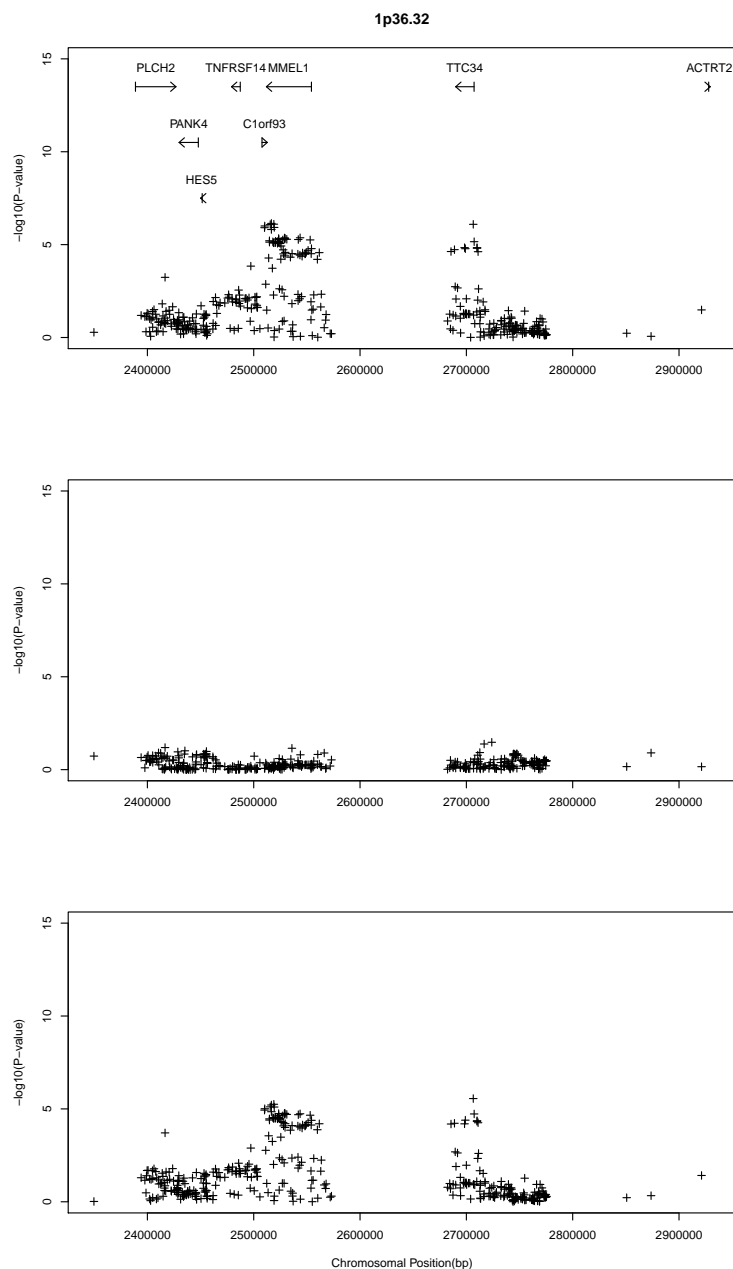


Figure S3: Single-locus 1-df Cochran-Armitage trend test results at the novel AITD susceptibility locus 3q27.3/3q28. The most disease associated SNP, rs13093110 ($P = 3.7 \times 10^{-8}$ in HT and GD patients/controls; Table 1), was located within *LPP*. The top panel — GD patients and controls; the middle panel — HT patients and controls; and, the bottom panel — GD and HT patients and controls.

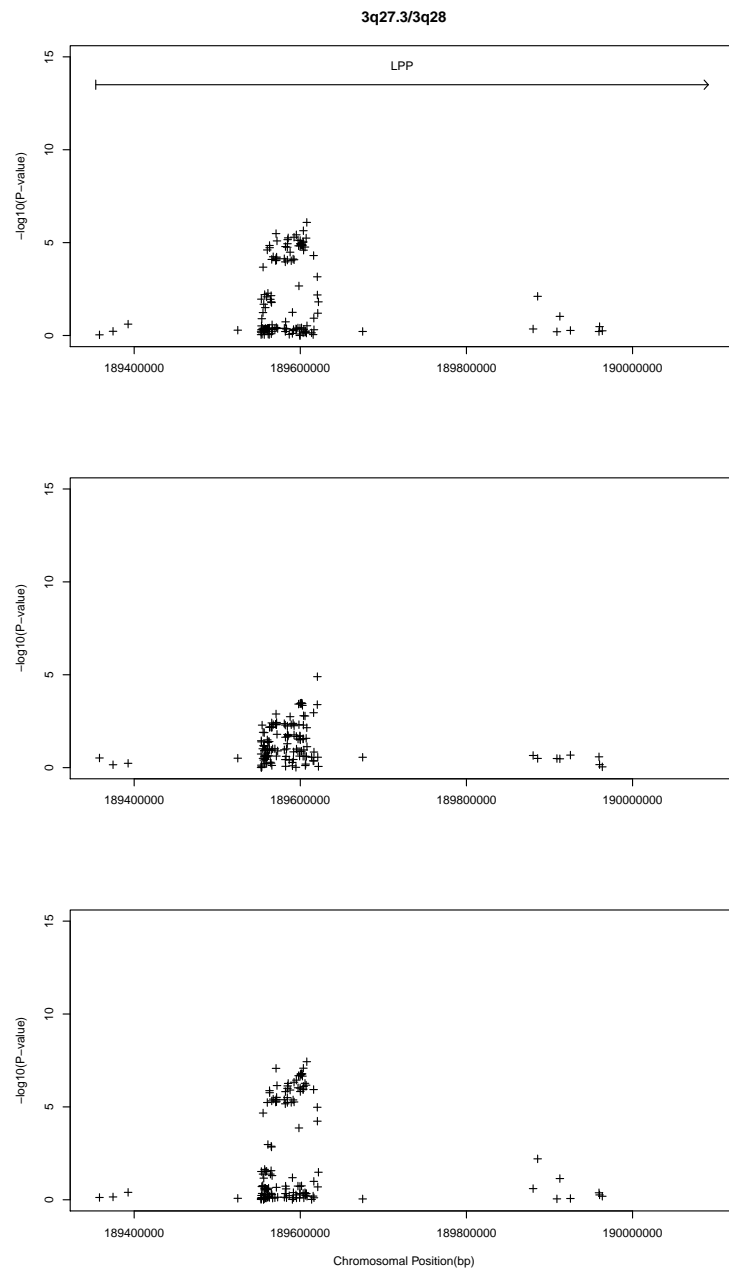


Figure S4: Single-locus 1-df Cochran-Armitage trend test results at the novel AITD susceptibility locus 6q15. The most disease associated SNP, rs72928038 ($P = 1.2 \times 10^{-7}$ in HT and GD patients/controls; Table 1), was located within *BACH2*. The top panel — GD patients and controls; the middle panel — HT patients and controls; and, the bottom panel — GD and HT patients and controls.

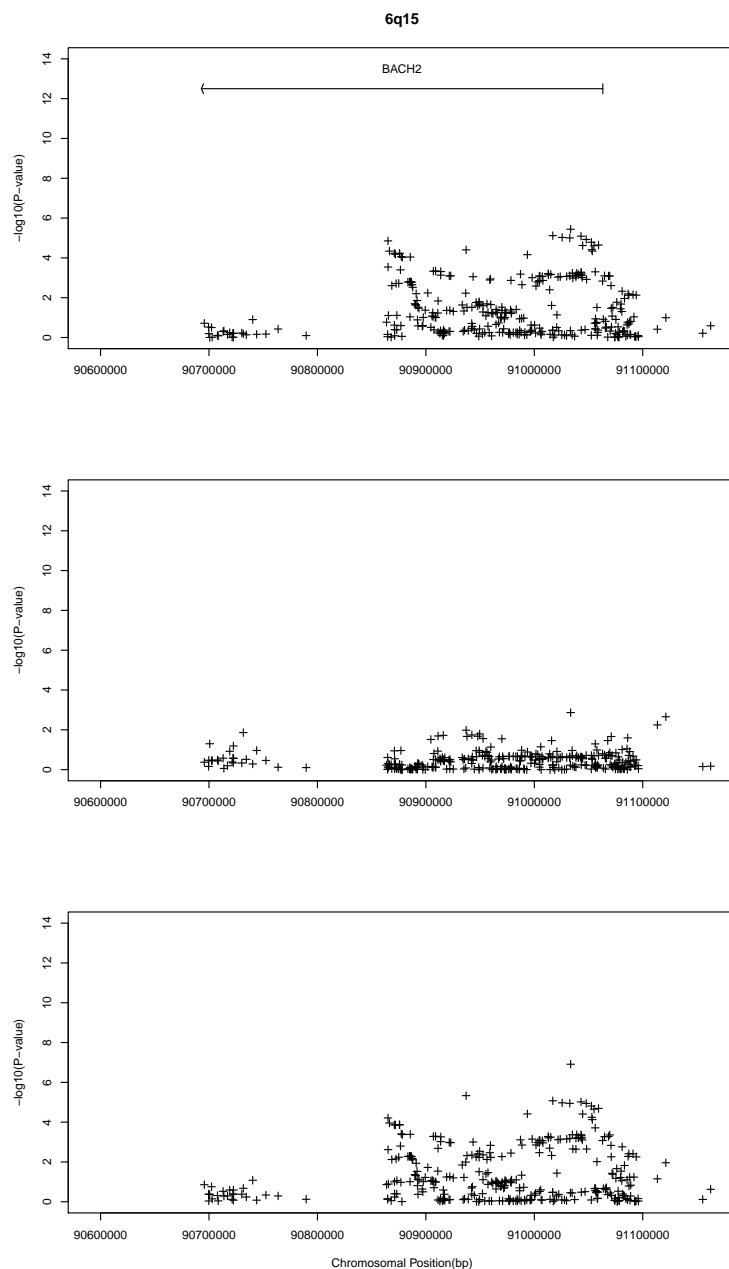


Figure S5: Single-locus 1-df Cochran-Armitage trend test results at the novel AITD susceptibility locus 12q12. The most disease associated SNP, rs57348955 ($P = 3.8 \times 10^{-8}$ in GD patients/controls; Table 1), was located within *PRICKLE1*. The top panel — GD patients and controls; the middle panel — HT patients and controls; and, the bottom panel — GD and HT patients and controls.

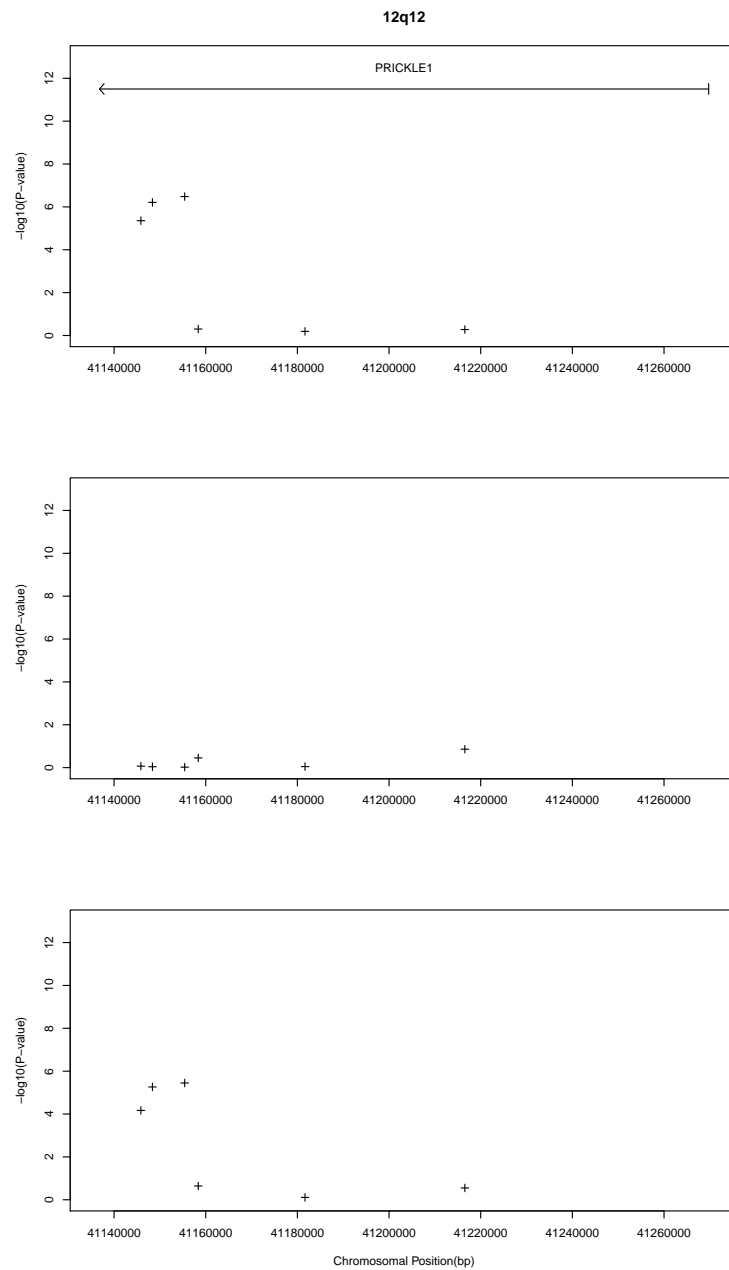


Figure S6: Single-locus 1-df Cochran-Armitage trend test results at the novel AITD susceptibility locus 16p11.2. The most disease associated SNP, rs57348955 ($P = 3.8 \times 10^{-8}$ in GD patients/controls; Table 1), was located 82.6 kb upstream of *ITGAM*. The top panel — GD patients and controls; the middle panel — HT patients and controls; and, the bottom panel — GD and HT patients and controls.

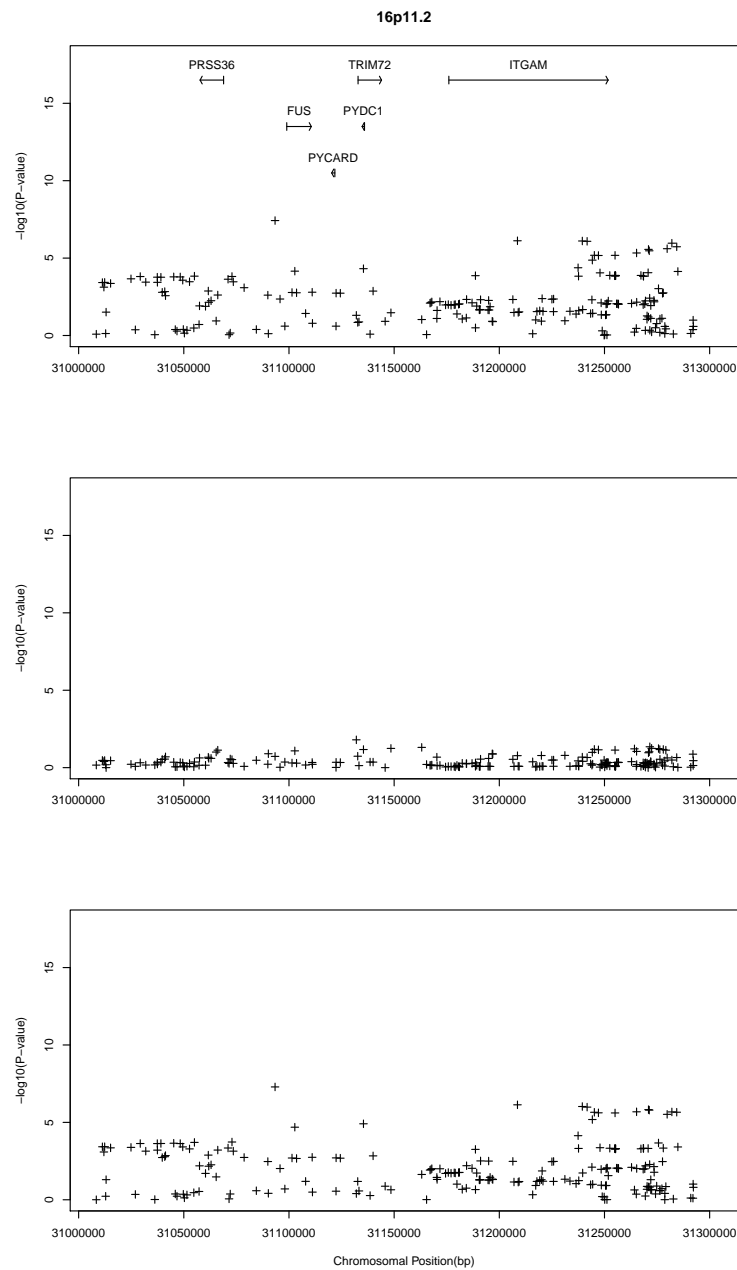


Figure S7: Single-locus 1-df Cochran-Armitage trend test results at the novel AITD susceptibility locus 2p25.1. The top panel — GD patients and controls; the middle panel — HT patients and controls; and, the bottom panel — GD and HT patients and controls.

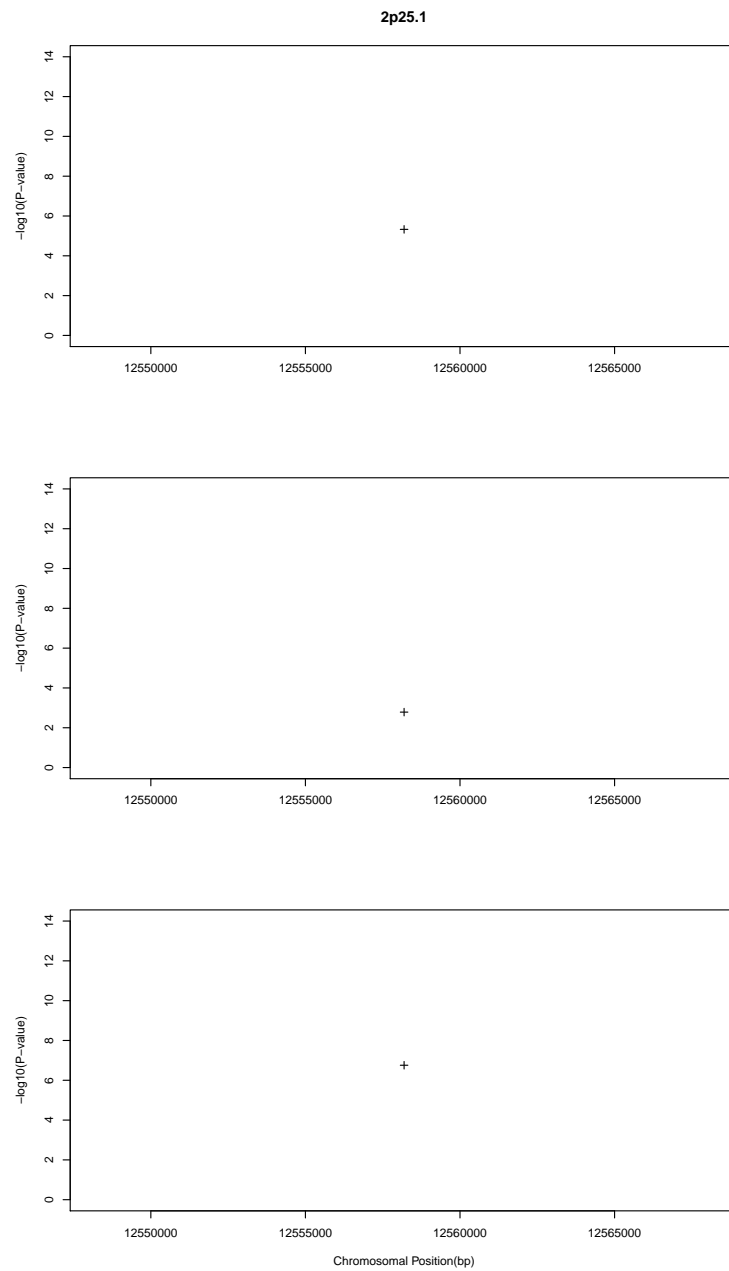


Figure S8: Single-locus 1-df Cochran-Armitage trend test results at the novel AITD susceptibility locus 11q21. The top panel — GD patients and controls; the middle panel — HT patients and controls; and, the bottom panel — GD and HT patients and controls.

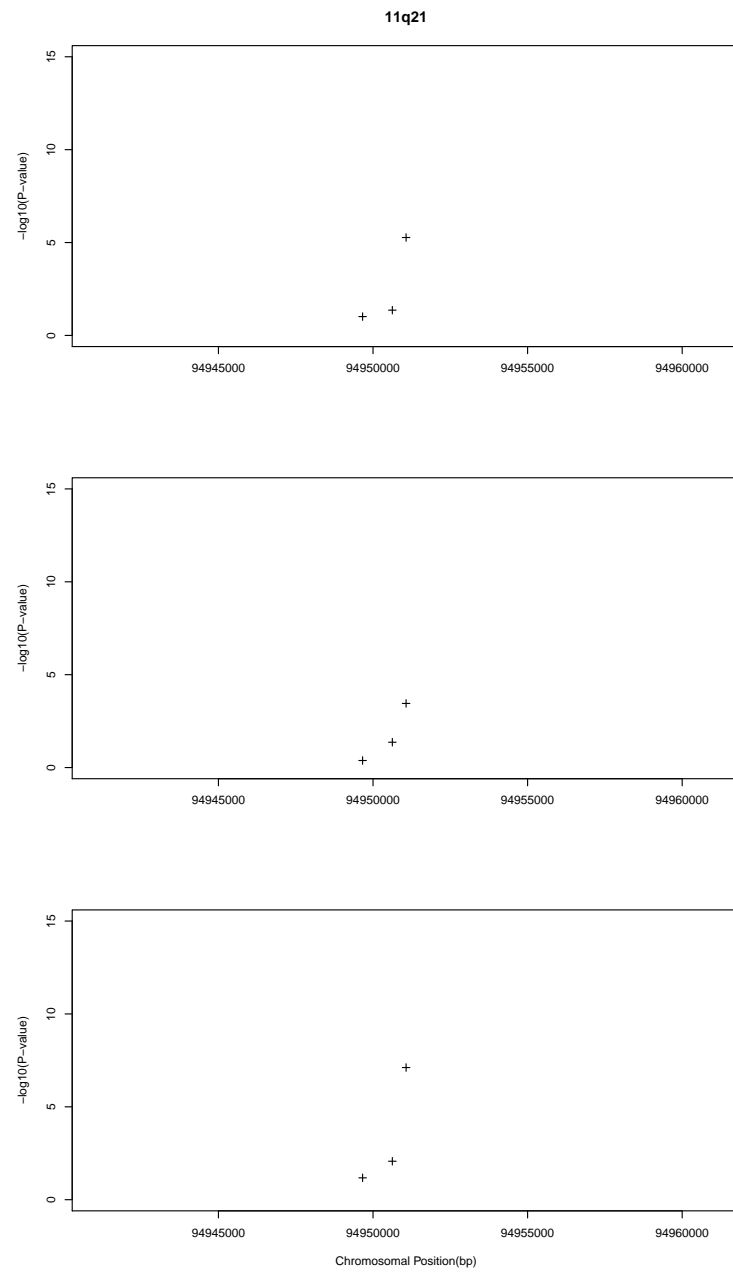


Figure S9: Per-sample call-rates versus heterozygosity across chromosomes 1 to 22 for WTSI control samples. Dashed lines denote the quality controls thresholds applied.

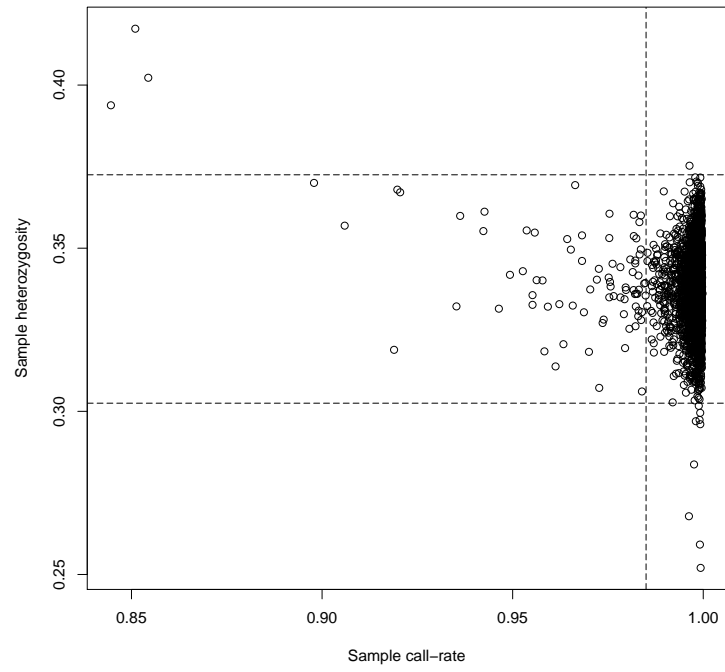


Figure S10: Per-sample call-rates versus heterozygosity across chromosomes 1 to 22 for UVA control samples. Dashed lines denote the quality controls thresholds applied.

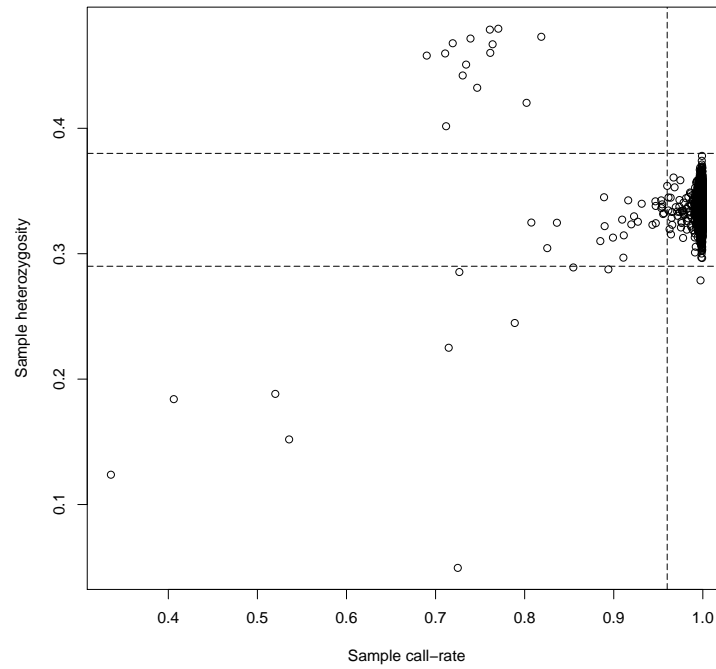


Figure S11: Per-sample call-rates versus heterozygosity across chromosomes 1 to 22 for AITD patient samples. Dashed lines denote the quality controls thresholds applied.

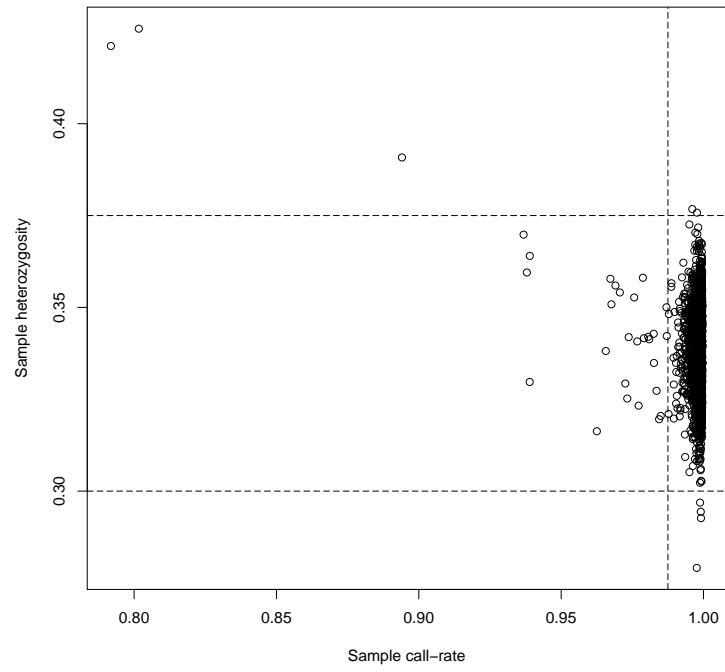


Figure S12: Ancestry clusters based on HapMap2 reference samples and SNPs available on the ImmunoChip that differentiated between the three HapMap populations (CEU, YRI and JPT+CHB) to derive two principal component scores for ancestry to exclude WTSI control subjects with substantial non-European ancestry. We excluded 18 WTSI controls subjects.

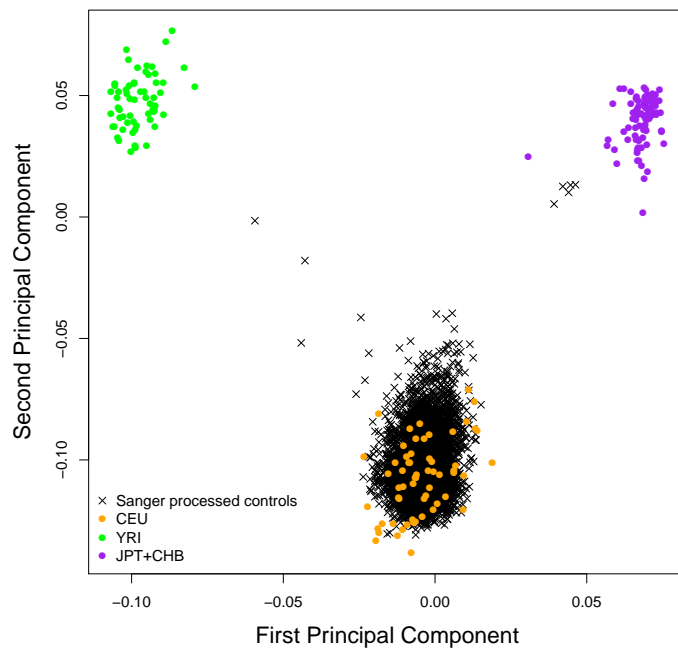


Figure S13: Ancestry clusters based on HapMap2 reference samples and SNPs available on the ImmunoChip that differentiated between the three HapMap populations (CEU, YRI and JPT+CHB) to derive two principal component scores for ancestry to exclude UVA control subjects with substantial non-European ancestry. We excluded five UVA control subjects.

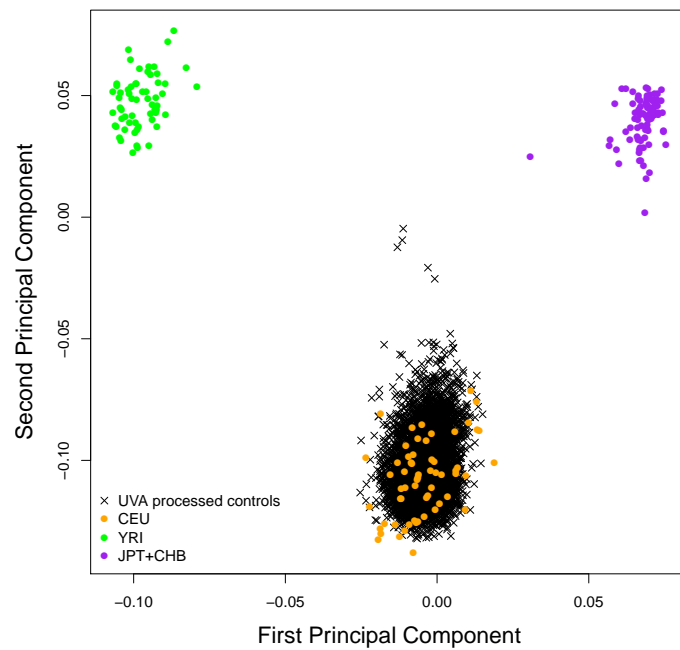


Figure S14: Ancestry clusters based on HapMap2 reference samples and SNPs available on the ImmunoChip that differentiated between the three HapMap populations (CEU, YRI and JPT+CHB) to derive two principal component scores for ancestry to exclude AITD patients with substantial non-European ancestry. We excluded three AITD patients.

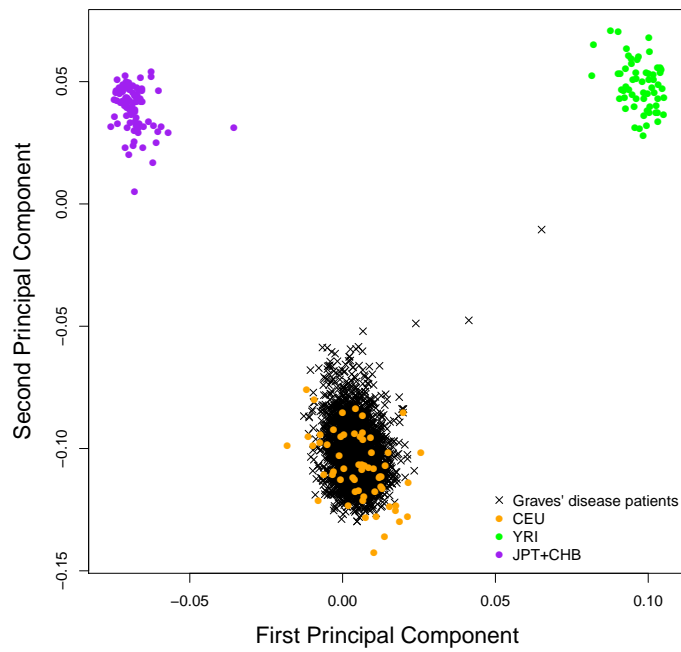
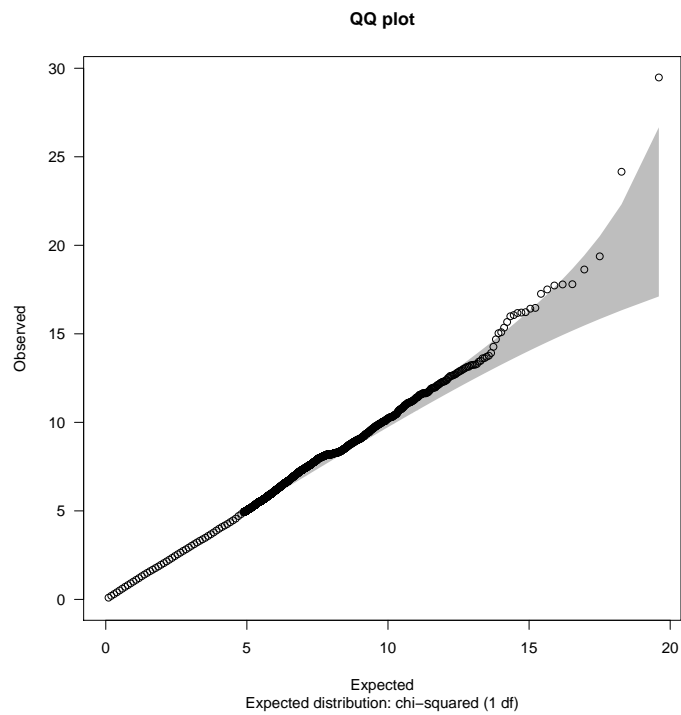


Figure S15: Quantile-quantile plot for the 1 degree-of-freedom association tests between WTSI and UVA control samples. The overdispersion factor (λ) of the 1-df association tests was 1.017.



References

1. Chu, X., *et al.* (2011) A genome-wide association study identifies two new risk loci for Graves' disease. *Nat Genet* **43**, 897-901.